Journal of Operation and Automation in Power Engineering

vol. XX, no. XX, Dec. 2022, Pages: XXXX (Proofed)

http://joape.uma.ac.ir

Development of an Adaptive Protection Scheme for Microgrid Operation Suitable for Grid-Connected and Islanded Mode

N. Kumar and D.K. Jain*

Department of Electrical Engineering, Deenbandhu Chhotu Ram University of Science and Technology, Murthal, Sonipat, Haryana, India.

Abstract*— *The integration of distributed generations (DGs) can disrupt the distribution system's radial configuration, leading to potential coordination issues with the existing protection scheme. Disparate operating modes of microgrids render traditional protection schemes ineffective and insecure. This highlights the need for alternative approaches to ensure the reliability and security of microgrids. To mitigate the relay coordination problem in microgrids, this paper puts forth a solution in the form of an adaptive protection scheme. The proposed method is based on fault current and integrates the use of adaptive numerical directional overcurrent relays (ANDOCRs). The proposed adaptive protection strategy encompasses a microgrid central protection controller (MCPC) equipped with communication capabilities. This feature enables MCPC to communicate with intelligent field electronics devices (IFEDs). The MCPC receives data from the IFEDs and updates the ANDOCRs' settings according to the operation mode. This paper suggests a modified objective function specifically tailored to tackle the nonlinear optimization problem for relay coordination in microgrids to strengthen the coordination between primary and backup relays. The proposed adaptive protection scheme also incorporates a quick online fault detection algorithm to identify the faulty feeder precisely. The proposed method is assessed for its performance using a highly unbalanced IEEE-13 node distribution system in MATLAB/Simulink.

***Keywords*—**Grid-connected, adaptive protection, microgrid, JAYA, relay coordination.

NOMENCLATURE

β	Miscoordination control parameter
ΔT_{mbp}	Operating time difference with CTI between relay pairs
$I_{fault,max}$	Maximum fault current
$I_{fault,min}$	Minimum fault current
$I_{fault,min}$	Phase fault current across all phases
OT_B	Operating time of backup relay
OT_P	Operating time of primary relay
W_i	Weight attributed to relay
α_1, α_2	Weight control factor
ANDOCR	Adaptive numerical directional over current relay
CNN	Convolutional Neural Network
COF	Conventional objective function
CTI	Coordination time interval
DER	Distributed energy resources
DG	Distributed generation
FREEDM	Future Renewable Electric Energy Delivery and Management
GA	Genetic Algorithm
GSO	Gravitational search algorithm
IFED	Intelligent field electronic device
LP	Linear programming
MCPC	Microgrid central protection controller
MOF	Modified objective function
OCR	Over-current relay
PCC	Point of common coupling
PSO	Particle swarm optimization
STI	Selective time interval
TDS	Time dial setting
THD	Total harmonic distortion
WOA	Whale optimization algorithm

Received: 29 Jun. 2023
Revised: 17 Nov. 2023
Accepted: 30 Dec. 2023
*Corresponding author:
E-mail: 16001002004naveen@dcrustm.org (N. Kumar)
DOI: 10.22098/joape.2024.13229.2004
Research Paper

1. INTRODUCTION

1.1. Research motivation

Microgrids are characterized by interconnected loads and DERs on a smaller scale and within a defined geographical area. Their popularity is increasing globally due to various factors. Microgrids offer several technical advantages, such as enhanced power supply reliability and optimized utilization of DER. This contributes to their growing presence in electricity networks worldwide. The progress and adoption of microgrids have gained momentum in the past two decades. The concept of an intelligent microgrid was initially introduced in the early 2000s [1, 2]. It has gained significant popularity due to its ability to accommodate and integrate DGs and RESs on a large scale.

This distribution system architecture offers numerous advantages, such as eliminating the need for transmission corridors and high-voltage distribution systems. This addresses the growing demand for electrical energy, enhancing power supply reliability, increasing resiliency and security of power supply for end-users, and improving energy utilization efficiency. However, microgrids also face various challenges due to their unique characteristics, operating modes, and integration of DERs. These challenges include ensuring fault prevention, addressing transient and dynamic control issues, managing bidirectional power flow, mitigating DERs loss of synchronism, addressing changes in fault current magnitude, and managing system inertia reduction.

Due to the unique characteristics of microgrids, traditional protection and control methods may not be adequate to ensure

their security. Therefore, specialized approaches for protection and control are essential in microgrid systems. Microgrids must have a robust protection mechanism that can effectively respond to issues within the microgrid and in the utility grid. If faults occur in the utility grid, the protection system should swiftly trip the circuit breaker at the PCC and disconnect the microgrid from the primary grid to ensure its isolation and prevent further disruptions. Addressing internal faults in microgrids requires a reliable protection system that can swiftly isolate the affected area while minimizing the disruption to the rest of the grid [3, 4]. However, developing such a protection architecture that can effectively operate in grid-connected and islanded modes presents a significant challenge. To tackle this challenge, researchers and experts in the field have made notable advancements, including developing innovative control techniques and sophisticated protection and fault detection systems.

Traditional protection schemes prove inadequate as they need more adaptability to adjust relay settings in response to network changes arising from DG integration. Given this, adaptive protection schemes are required to accommodate these real-time changes. In summary, the motivation for research in adaptive protection for microgrids arises from the unique challenges and opportunities presented by these dynamic and evolving energy systems. Adaptive protection ensures microgrids' reliable and secure operation in the face of changing conditions and emerging technologies.

1.2. Literature review

Addressing the challenge has seen significant progress from researchers and field experts, encompassing pioneering control techniques and advanced protection and fault detection methods in the literature. Various research studies have explored different approaches to provide solutions for adaptive protection coordination.

Louie et al. [5] explored the implementation of monitoring systems in islanded microgrid systems in Kenya and Zambia. Their study highlighted the issues in microgrid applications and suggested solutions. In the protection scheme [6], the primary objective is to identify the type of fault in the system. Subsequently, THD is employed to distinguish between the faulted zones in grid-connected mode only. This approach faces limitations when the grid enters islanding mode or when significant operational changes occur. In such scenarios, the fault type identification and fault zone differentiation based on THD may become less accurate or unreliable.

Researchers proposed a solution for enhancing protection coordination using the selection of OCR curves [7]. To achieve this, a hybrid approach combining GA and LP is utilized to determine the optimal settings and curves for the relays. One of the disadvantages of OCR curve selection is the complexity and difficulty of determining the appropriate curve for a specific application. The selection process involves considering various factors such as fault current magnitude, fault type, system impedance, and coordination with other protective devices. This complexity can lead to errors or suboptimal curve selection, potentially compromising the reliability and effectiveness of the protection scheme. Additionally, the manual adjustment of OCR curves can be time-consuming and labor-intensive, especially in large-scale power systems with numerous relays.

In [8], a relay coordination method is proposed for a complex power system, utilizing a hybrid metaheuristic algorithm based on the WOA. The coordination problems become complicated in microgrid scenarios, so this approach is not limited to microgrids. One of the main disadvantages of WOA is its high computational complexity and time-consuming nature. WOA involves a large number of iterations for evaluating fitness functions for a large population. This can significantly increase the computational cost. As a result, WOA may not be suitable for problems that have strict time constraints or require real-time optimization. Additionally, WOA's performance heavily relies on parameter settings, such as the population size, convergence criteria, and exploration-exploitation balance.

M. A. Haj-Ahmed *et.al* proposed a groundbreaking approach to power system protection coordination by utilizing a multi-agent system methodology [9]. One of the major drawbacks of the multi-agent approach in relay protection is the growing complexity and computational burden. It arises due to managing multiple agents. As the number of agents rises, ensuring effective communication and coordination between them becomes increasingly difficult and resource-intensive. This can result in higher computational efforts and longer processing times. This can potentially impact the real-time performance of the relay protection system. If there are communication issues or delays, it can affect the coordination and response of the agents which leads to suboptimal or incorrect protection actions. Another method proposed in [10] emphasizes the use of communication systems to facilitate protection coordination in grid-connected and islanded modes. However, a limitation of this approach is that it is primarily applicable to medium-voltage microgrids, potentially restricting its effectiveness in high or low-voltage microgrid environments. In [11], a pioneering approach has been proposed for microgrid protection, incorporating communication assistance. H. F. Habib *et.al* [12] introduce an adaptive protection scheme that leverages energy storage devices to improve resiliency during communication outages.

Studies in [13] and [14] underscore the crucial role of sensitivity and selectivity in protection coordination when integrating DGs. A specialized adaptive protection scheme has been introduced in [15] which is primarily focused only on distribution systems. This scheme offer tailored protection solutions for grid-connected scenarios with high penetration of DGs only. However, its applicability is limited to this specific mode of operation.

In [16], an adaptive protection strategy is proposed for microgrids to tackle coordination issues among numerical directional overcurrent relays during fault events. The strategy incorporates a hybrid GA and utilizes a conventional objective function to optimize the relay coordination process. A limitation of the COF in relay coordination problems is their inherent inability to effectively handle the intricate and dynamic characteristics of the microgrids. Due to the unique operating conditions and varying system configurations of microgrids, COF falls short of providing optimal and adaptable coordination solutions. This leads to potential issues such as miscoordination and insensitivity in response to changing conditions. As a result, the COF may not fully capture the specific requirements and intricacies of microgrids, leading to suboptimal relay coordination and potential reliability concerns.

In [17] proposed an adaptive inverse time overcurrent protection method for low voltage microgrid. But this scheme does not involve any relay coordination method.The method proposed in [18] emphasizes the use of non-standard characteristics to facilitate protection coordination in microgrid. However, utilization of DOCRs with non-standard characteristics could result in compatibility problems within the microgrid protection system. Additionally, employing non-standard characteristics might restrict the system's flexibility for future upgrades and scalability. In [19], a pioneering approach has been proposed for networked microgrid protection using multiple setting groups. Networked microgrids make it difficult to coordinate protection devices since each setting group needs to be carefully set up to provide proper fault discrimination and selectivity. The reliability and stability of the microgrids may be compromised by inappropriate settings or ignored interactions between various groups that result in improper or delayed fault clearance. Relays with several setting groups may require more complex and capable equipment, which could increase expenses. A. Ataee-Kachoee *et.al* [20] introduce an adaptive protection scheme that incorporates dual-setting directional overcurrent relays based on limited independent relays

setting groups. When the number of independent relays' setting groups is limited, the system's ability to adapt to dynamic changes in the microgrid may be compromised. Any discrepancies or inaccuracies in the system models might lead to suboptimal or ineffective coordination. Therefore, for any optimized adaptive coordination, accurate and up-to-date system models are crucial. An hybrid Differential Evolution and Interval linear programming [21] based optimal coordination of DOCR for grid-connected and isolated network modes. The draw back of this method is that it is computationally intensive and time-consuming, especially for large and complex optimization problems. H.Shad *et.al* [22] proposed a novel truth table based optimal protection coordination for directional overcurrent relays in meshed distribution networks with DG. This scheme introduces a user-defined setting for numerical DOCRs to reduce the total relay operation time while taking into account the existing constraints.

A novel protection strategy has been developed in [23] utilizing digital DOCRs and dual-setting digital DOCRs within the distribution network, considering the integration of RESs and energy storage systems. Naveen *et.al* [24] suggests an adaptive protection scheme designed to address the coordination problem of DER in a microgrid with multiple PCCs.Managing protection relays and ensuring their coordination becomes more complex as the number of PCCs increases. Coordinating relays to operate in a coordinated manner across multiple PCCs can be challenging, leading to potential misoperations or delays in fault clearance.

In [25] an adaptive protection strategy designed for the FREEDM system. This proposed approach utilizes a CNN as its foundation. As FREEDM systems rely heavily on communication networks and digital technologies, they may be vulnerable to cyber security threats. Protecting these systems from cyber attacks becomes a significant concern. Ensuring seamless communication and coordination between the FREEDM system and legacy equipment may require additional effort and investment. Author in [26] has proposed an unsupervised learning technique for protection of microgrid. To achieve optimal performance, unsupervised learning models often require extensive fine-tuning. The process of adjusting the model to meet specific coordination goals becomes more challenging and time-consuming due to the absence of well-defined target outcomes. So, it is crucial to carefully validate and test unsupervised learning-based coordination techniques under various microgrid conditions.

1.3. Novelty and main contribution of paper

Several researchers in the above literature have approached relay coordination problems using different optimization functions, including linear and non-linear formulations. In the literature, some researchers have proposed adaptive protection strategies specifically cater to grid-connected mode but may fail to perform optimally when microgrids transit into islanded mode. On the other hand, adaptive protection schemes that accommodate both modes often rely on fixed primary and backup relay pairs. However, this fixed configuration can introduce dead zones in the system, leading to suboptimal protection as fault currents may be missed from certain paths.Many researcher has performed the relay coordination problem using different metaheuristic techniques which needs expertise to tune their parameter.To address these limitations, this research paper introduces a straightforward and communication assisted efficient adaptive protection scheme suitable for grid connected and islanded mode of operation.

The novelty of this work can be summarized as follows:

- The proposed adaptive protection scheme incorporates a quick fault detection algorithm to precisely identify the faulty feeder.
- The scheme also present an online algorithm to dynamically calculate the operating parameter of relay i.e is TDS and CPS considering different modes of operation, location of DGs, fault type and fault location.
- In addition to this, TDS and CPS are obtained using JAYA optimization technique that requires minimal parameter tuning, making it a robust and reliable tool for the optimization task.
- A modified objective function is proposed for microgrid to mitigate miscoordination issues and minimize discrimination time.
- Communication assistance is incorporated to enhance coordination among ANDOCRs. The proposed algorithm has the ability to modify the relay pair combinations stored in the offline relay programming module during transition from grid connected mode to islanded mode or vice versa for better selectivity and maximum protection.

The paper is divided into multiple sections to facilitate understanding. Section 1 provides a summary of prior research and introduces the specific work presented in this paper. In Section 2, problem formulation for relay coordination in microgrids is thoroughly discussed. Section 3 presents the implementation details of the proposed scheme. Section 4. gives an overview to the test system detail. The results and sensitivity analysis are comprehensively discussed in Section 5. Finally, Section 6 concludes the findings and outcomes of the paper.

2. PROBLEM FORMULATION

The coordination of ANDOCRs is a critical component in any protective strategy. Selecting the appropriate relay configuration ensures that the faults in the protected feeder are cleared first by the associated primary relays. If the primary relays fail to clear the faults, the backup relays come into operation after a certain time delay known as the CTI or STI [27]. The coordination problem is defined as achieving a high level of selectivity among protective devices [28]. The relay settings, namely CPS and TDS play a crucial role in determining the operating time of each relay. The objective of optimal coordination is to determine the optimal relay settings that minimize the total operating time of primary relays while satisfying the given constraints [29]. The most commonly used objective function in the literature is the total weighted sum of primary relay operating times, which has been widely employed and given in Eq. (1).

$$\text{Minimize COF} = \sum_{1}^{n} Wi.Ti. \tag{1}$$

Where,

W_i= weight attributed to the relay R_i's operating time, and generally, its value is taken as one [28].

N = no of relays.

T_i = operating time of relay R_i.

To address the issues of miscoordination and insensibility highlighted in [12], a new objective function is proposed for overcurrent relay coordination [30]. The proposed MOF aims to overcome the limitations of the existing COF and improve coordination performance.

$$\begin{matrix}\min\left(CPS_i,\, TDS_i,\, MOF\right) = a_1 \sum_{i}^{m} \sum_{j} T_{ij}^2 + \\ a_2 \sum_{p=1}^{mp} \left[\Delta T_{\text{mbp}} - \beta\left(\Delta T_{mbp} - |\Delta T_{mbp}|\right)\right]^2\end{matrix}, \tag{2}$$

$$\Delta t_{mbp} = t_{ki} - t_{ij} - CTI. \tag{3}$$

where Δt_{mbp} is the operating time difference with CTI between the relay pairs, and m_p is the number of primary and backup relay pairs. The index 'p' represents each specific primary/backup relay pair, ranging from 1 to m_p. Additionally, the weighting factors α_1 and α_2 are introduced to control the importance assigned to the first and second terms of the MOF. These factors are designed to account for miscoordination and ensure appropriate weighting of the objective function components.

By increasing the value of β, the level of miscoordination in ANDOCR is reduced, but it may lead to an increase in the operational time of the relays. Therefore, it is important to find the optimal value of β that minimizes miscoordination while keeping the relay operation times within acceptable limits. The reliable protection of microgrids heavily relies on the efficient coordination of ANDCORs. In the context of microgrid, the challenges faced can be framed as an optimization problem. The goal is to minimize the total operation time of all relays while meeting specific constraint requirements [30, 31]. CTI between primary and backup relay is given as:

$$CTI = T_{kj} - T_{ij}\ , \qquad i = 1, .., m. \tag{4}$$

Where T_{kj} and T_{ij} are the operating time of the backup relay and primary relay respectively for a fault inside a feeder protected by i^{th} primary relay for a fault at j. The inequality constraint given for CTI is as follows:

$$CTI \ \geq \ CTI_{min}. \tag{5}$$

The distinctive value of CTI_{min} is 0.2 to 0.3 s [31]. The settings for TDS and CPS must fall within specified limits. The upper and lower bounds for these settings can be defined as follows:

$$TDS_i^{min} \leq \ TDS_i \leq \ TDS_i^{max} \qquad i = 1, .., m, \tag{6}$$

$$CPS_i^{min} \leq \ CPS_i \leq \ CPS_i^{max} \qquad i = 1, .., m. \tag{7}$$

where $TDS_{i,}^{min} TDS_i^{max}$ and $CPS_{i,}^{min} CPS_i^{max}$ are the minimum and maximum limits of the time dial setting and current plug setting, respectively. The operating time of each primary relay is accomplished by:

$$T_{ij}{}^{min} \leq \ T_{ij} \leq T_{ij}{}^{max} \qquad i = 1, .., m. \tag{8}$$

Where $T_{ij}{}^{min}$ and $T_{ij}{}^{max}$ are the minimum and maximum operating times of primary relay i for fault at j.

3. PROPOSED ADAPTIVE PROTECTION STRATEGY

An adaptive protection scheme refers to an online process that adjusts the protective response based on changing system conditions or requirements. It typically operates automatically but may involve timely human intervention [32]. Adaptive protection encompasses protective relays with dynamically adjustable settings and reliable communication infrastructure. The ultimate goal of any protective scheme is to isolate only the faulty component from the rest of the system. With these requirements in mind, the proposed adaptive protection strategy includes a microgrid central protection controller capable of communicating with intelligent field electronics devices. IFEDs receiving data from them, and updating the settings of the ANDOCRs. The proposed algorithm is explained in the following subsections.

3.1. Measurement of actuating parameter

Accurate measurement of the actuating input serves as the initial requirement for any protective scheme. To fulfill this requirement, the currents of all three phases are measured from all integrated SBDGs as well as primary utility sources. Alongside current measurement, the measurement system also incorporates a signal that indicates the current direction in each protected line segment breaker.

3.2. Pre-calculated protection settings and data storage

The determination of protective settings relies on a pre-calculated table of values derived from various anticipated scenarios. This approach involves assessing the number of viable microgrid configurations, which is primarily determined by the number of switches and the states of the SBDGs feeding into the system. The offline pre-calculated task encompasses conducting short circuit analysis for various fault types at different locations in the microgrid. This task also involves defining constraint limits and selecting primary and backup relay pairs for each fault location and operating mode.

The outcome of the offline pre-calculated task is the generation of an event table, which provides a comprehensive list of possible outcomes. To maintain accuracy, any significant changes in the system configuration, load, and DGs need to be promptly updated in the database. With the advanced computing power and ample memory capacity of today's systems, offline calculations and data storage are no longer a major concern. The fast-processing capabilities of modern computers ensure efficient execution of calculations, while the expanded memory capacity allows for seamless storage of data.

3.3. Sensing, identification of fault type, and fault location

Under normal operating conditions, the summation of current phasors obtained from all SBDGs and utility main sources should equate to the net load of the system. In the event of a fault or abnormal condition, this sum of currents will surpass the total load, triggering the detection of fault current in the microgrid. This initiates the sensing of fault current in the distribution system. If the net sum is zero, the fault is in DG because the DG is outside the monitored zone. The net fault current after detecting the fault can be determined as given below.

$$[I_{fault,abc}] = \sum_{j=1}^{n} [I_{fault,abc}]_{sourcej} \tag{9}$$

In Eq. (9), the left-hand side term represents the total phase fault current across all three phases. On the right-hand side, the term corresponds to the fault current contribution from the 'j' source across the three phases. The parameter 'n' represents the total number of generating sources, including the utility main source. The offline database stores the pre-calculated short circuit currents for each phase and fault type, encompassing all energy sources and buses. Additionally, the online system provides real-time access to the current supplied by each source. The total fault current is obtained by aggregating the contributions from all connected sources. In the case of a specific fault type, when the fault location transitions from one node (i) to another node (j) along a particular line section ($i - j$), the fault current supplied by any source can either steadily increase from $I_{fault,min}$ to $I_{fault,max}$ or steadily decrease from $I_{fault,max}$ to $I_{fault,min}$. This indicates that the change in fault current within a line section falls between the values obtained for the fault locations i and j, considering a specific fault contributed by source k. The complete proposed adaptive protection algorithm flowchart is illustrated in Fig. 1.

The algorithm initiates with the measurement of three-phase current from all connected sources, including the primary utility source. If the sum of currents is zero, it indicates that the fault is inside the DG and requires manual clearing of the fault. If the sum of currents is not zero, it means either the transient persists or a temporary fault. If the fault current magnitude is much higher than the total load currents and exists for a particular period, then it indicates the existence of faults. The fault type identification is based on the sequence components' presence [33]. The algorithm is set up to recognize positive sequence components for three-phase faults. In contrast, negative and zero sequence components are detected for single-phase and ground faults, respectively.

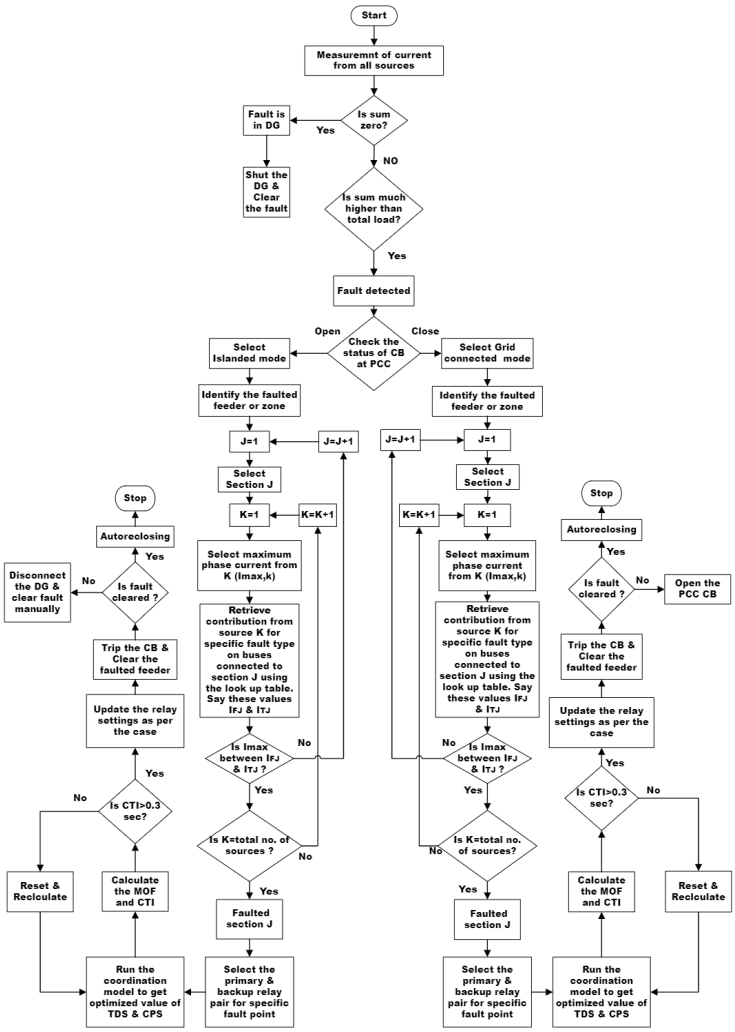

Fig. 1. Proposed Adaptive protection scheme.

The actuating quantity is continuously sent to the MCPC through a communication channel by IFEDs. After witnessing the fault, MCPC checks for the operating modes. If the PCC circuit breaker opens, a signal is sent to the MCPC. This signal will trigger the algorithm to enter either grid-connected or islanded mode. After detecting the operating modes, the MCPC, with the help of the online measured parameters and offline stored database, the algorithm identifies the type of fault and faulted section as mentioned in Fig. 1.

After detecting the fault location and mode of operation, MCPC selects the primary and backup relay pairs from the saved database according to Table 2. Now MCPC runs the coordination model to get the optimal set of values of TDS and CPS for a particular relay pair. If CTI obtained from the MOF is following the coordination criterion, then it updates the new setting of relay pairs depending upon the mode of operation. The time it takes to update the relay settings is resolute on the MCPC processor speed in the field as well as the communication route. If the CTI criterion is not filled then the algorithm resets and recalculates the value of TDS and CPS. The relay would deliver a trip signal to isolate the faulted section and DG in this zone after the faulted part was sited. The offline database already has information about the breakers that must be tripped to isolate a specific section. If the fault is not cleared, then DGs are disconnected, and the fault is cleared manually. The online and offline task performed by the proposed scheme is shown in Fig. 2.

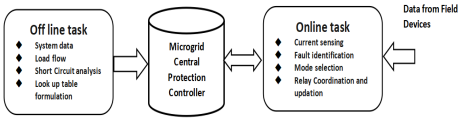

Fig. 2. Online and offline tasks performed by the proposed scheme.

4. TEST SYSTEM DESCRIPTION

The IEEE developed a 13-node radial test feeder to replicate an entire distribution network with imbalanced loading conditions, allowing researchers to validate their study findings [34], [35]. This test system consists of distribution lines spanning a total length of 2.49 km and operates at a voltage of 4.16 kV with a frequency of 60 Hz. Additionally, the system incorporates a voltage regulator, a 115/4.16 kV Y transformer, and a 4.16/0.480 kV Y-Y step-down transformer. Various points within the system are connected to eight unbalanced spot loads and two distributed loads. To establish a microgrid, three SBDGs units, each with a capacity of 1 MVA, are connected at nodes 633, 675, and 680. To ensure optimal protection, the modified IEEE 13-node distribution system incorporates a total of 24 ANDOCRs positioned

Table 1. CT ratios.

Relay No.	CT ratio
R_1, R_2, R_3, R_4	500/5
R_5, R_6, R_7, R_8, R_{15}, R_{16}, R_{17}, R_{18}	1000/5
R_9, R_{10}, R_{21}, R_{22}, R_{23}, R_{24}	1200/5
R_{11}, R_{12}, R_{13}, R_{14}, R_{19}, R_{20}	200/5

at various locations. Each relay is equipped with a specific current transformer rating, as indicated in Table 1.

Fig. 3 illustrates eleven distinct locations along the distribution line where faults can occur, including nodes and sections within the line.

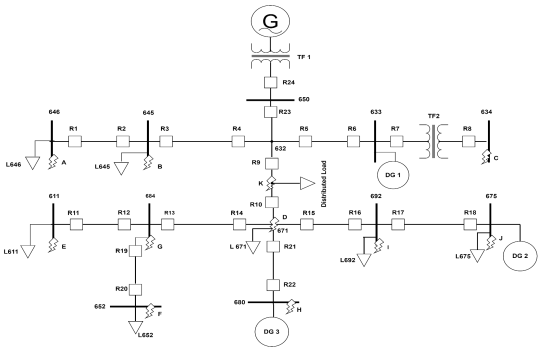

Fig. 3. Modified IEEE-13 node radial distribution system.

To ensure comprehensive protection, each feeder within the system is equipped with primary relays, complemented by backup relays for added security. Table 2 illustrates the corresponding pairs of primary and backup relays. Depending on the specific fault location and the operating mode (grid-connected or islanded), different relay configurations are employed. For example, at fault point A, in both modes, the primary relay R_1 is paired with the backup relay R_2. In the case of fault point D, R_{10}, R_{15}, and R_{21} are primary relays, backed up by R_9, R_5, R_{16}, and R_{22} respectively in grid-connected mode. However, in islanded mode, the backup relays for the same fault point are R_5, R_{16}, and R_{22}.

The relay pairings are carefully designed to ensure comprehensive protection throughout the microgrid. The relay programming module stores an offline database containing all the relay pairs for different fault locations.

5. RESULTS AND DISCUSSION

In order to evaluate the effectiveness of the suggested adaptive protection strategy, multiple scenarios are simulated for both operational modes. The optimal configurations for each mode are determined using the JAYA optimization technique [36]. The outcomes of these simulations are presented and discussed in the following subsections to provide a comprehensive analysis.

5.1. Grid connected mode

In this operational mode, the MCPC checks the status of the PCC circuit breaker and triggers the grid-connected mode settings based on the algorithm proposed. Fault currents are measured for single-phase feeders, two-phase feeders, and three-phase feeders.

A) Single phase feeder

A single-phase feeder runs from node 684 to node 611. To evaluate the system's response, a single phase-to-ground fault is simulated at the far end of the feeder, specifically at fault point E located at node 611, occurring at 0.5 seconds. Referring to the stored database for fault point E, it is determined that the primary relay R_{11} and backup relay R_{12} will be in active mode. For primary relay R_{11}, the optimized values of TDS and CPS result in a tripping time of 0.625 seconds. If the primary protection fails, relay R_{12} will trip after the CTI.The measured fault current and the tripping time of relay R_{11} are depicted in Fig. 4 and Fig. 5, respectively. Figs. 6 and 7 showcased the fault current and tripping time of the backup relay. CTI obtained in this case is 1.7 sec.

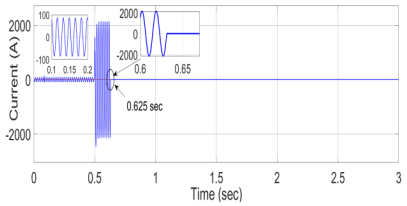

Fig. 4. Fault current and tripping time of primary relay R_{11}.

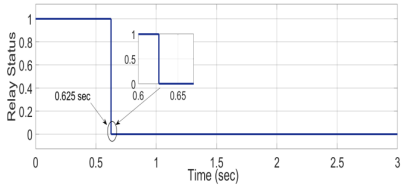

Fig. 5. Tripping Status of primary relay R_{11}.

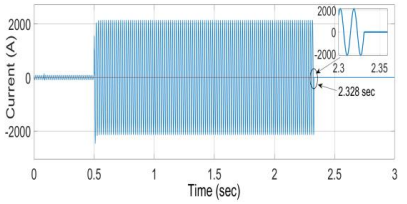

Fig. 6. Fault current and tripping time of backup relay R_{12}.

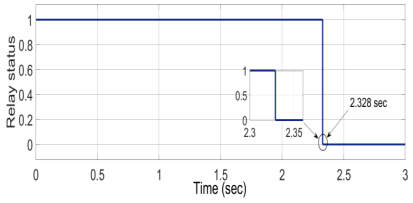

Fig. 7. Tripping status of backup relay R_{12}.

The CTI values obtained from JAYA optimization for all relay pairs are displayed in Fig. 10, with the minimum value being 0.3 seconds. There is no miscoordination occurred in grid-connected mode. Table 3 showcases the operating time of both primary and backup relays at different fault points. The optimized values of TDS and CPS for various relays are illustrated in Fig. 8 and Fig. 9, respectively.

B) Two-phase feeder

The investigation of the proposed algorithm's performance for an LL-G fault at fault point A is revealed here. The fault current is solely generated by the three SBDGs and the primary grid side. Due to the fault's occurrence at the feeder's farthest end, both primary relay R_1 and backup relay R_2 observe the fault current in only one direction. The performance of relay R_1 and relay R_2 is visualized in Figs. 11 to 14. In this particular case, the obtained CTI is 1.07 sec.

Table 2. Primary and backup relay pairs for Grid-connected and islanded modes.

Fault Point	Radial mode		Grid Connected mode		Islanded mode	
	P	***B***	***P***	***B***	***P***	***B***
A	R_1	R_2	R_1	R_2	R_1	R_2
B	R_3	R_4	R_3	R_4	R_3	R_4
C	R_8	R_7	R_8	R_7	R_8	R_7
D	R_{10}	R_9	R_{10}	R_9, R_5	R_{10}	R_5
			R_{15}	R_{16}	R_{15}	R_{16}
			R_{21}	R_{22}	R_{21}	R_{22}
E	R_{11}	R_2	R_{11}	R_{12}	R_{11}	R_{12}
F	R_{20}	R_{19}	R_{20}	R_{19}	R_{20}	R_{19}
G	R_{13}	R_{14}	R_{13}	R_{14}	R_{13}	R_{14}
H	R_{22}	R_{21}	R_{22}	R_{21}	R_{22}	R_{21}
I	R_{16}	R_{15}	R_{16}	R_9, R_{22}	R_{16}	R_{15}
			R_{17}	R_{18}	R_{17}	R_{18}
J	R_{18}	R_{17}	R_{18}	R_9, R_{22}	R_{18}	R_{17}
K	R_9	R_{23}	R_9	R_{23}, R_6	R_9	R_6
			R_{10}	R_{18}, R_{22}	R_{10}	R_{18}, R_{22}

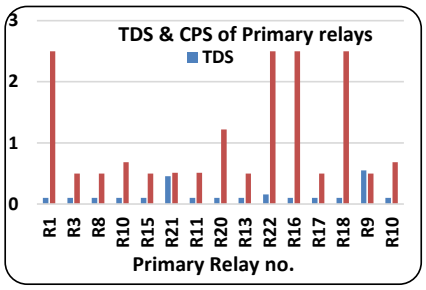

Fig. 8. Optimized values of TDS and CPS of primary relay.

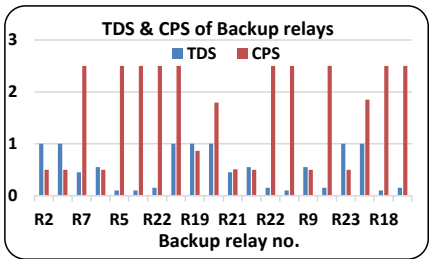

Fig. 9. Optimized values of TDS and CPS of backup relays.

C) Three-phase feeder

Although this type of fault occurrence is rare, the results obtained are crucial for selecting appropriate protective devices due to the generation of the highest magnitude of short circuit current. To simulate a three-phase bolted fault, fault location I is used. The fault current is contributed by all the DGs and the primary utility but from different directions. Therefore, it is essential for the directional elements integrated into the ANDOCR to function effectively in discriminating the fault direction.

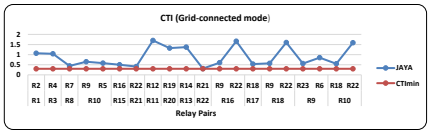

Fig. 10. CTI for all relay pairs in grid-connected mode.

To ensure network security and maintain reliability, the primary and backup relays are carefully chosen. This selection aims to minimize network disconnection while efficiently clearing the fault. Relay R_{16} is designated as the primary relay for currents originating from DG1, DG3, and the primary grid. The relays R_9 and 22 serve as backup relays. The performance of the relays

Table 3. Operating time of Primary and backup relays in grid-connected mode.

Fault Point	***P***	OT_P	***B***	OT_B
A	R_1	0.184	R_2	1.260
B	R_3	0.115	R_4	1.156
C	R_8	0.132	R_7	0.577
D	R_{10}	0.158	R_9	0.812
	R_{15}	0.273	R_5	0.738
			R_{16}	0.782
	R_{21}	1.422	R_{22}	1.833
E	R_{11}	0.125	R_{12}	1.828
F	R_{20}	0.162	R_{19}	1.491
G	R_{13}	0.114	R_{14}	1.483
H	R_{22}	0.437	R_{21}	0.756
I	R_{16}	0.223	R_9	0.823
			R_{22}	1.88
	R_{17}	0.276	R_{18}	4.041
J	R_{18}	0.246	R_9	0.823
			R_{22}	1.851
K	R_9	0.705	R_{23}	1.276
	R_{10}	0.255	R_6	1.556
			R_{18}	0.806
			R_{22}	1.851
Total Operating Time		4.82 sec		24.38 sec

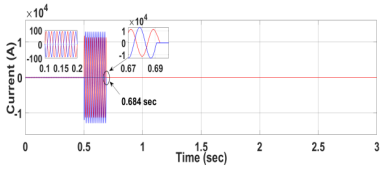

Fig. 11. Fault current and tripping time of primary relay R_1.

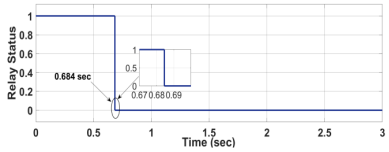

Fig. 12. Tripping status of primary relay R_1.

in this scenario is effectively captured in Figs. 15 to 20, which provides detailed information on the tripping time and status of the relays. These figures offer a comprehensive understanding of how the relays function and respond in a given situation.

The LLL-G fault is incepted at 0.5 sec. primary relay R_{16} trips at 0.723 sec with optimum value of TDS=0.1 and CPS=2.5. The tripping time of R_{16} is shown in Fig. 15. In case if failure

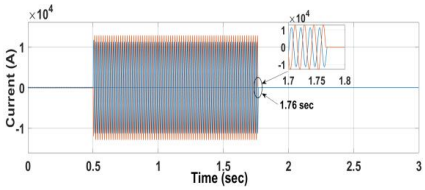

Fig. 13. Fault current and tripping time of backup relay R_2.

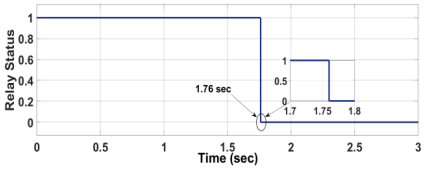

Fig. 14. Tripping status of backup relay R_2.

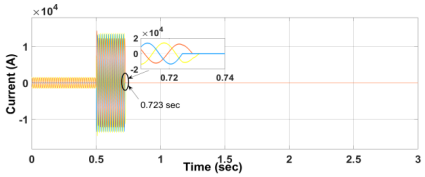

Fig. 15. Fault current and tripping time of primary relay R_{16}.

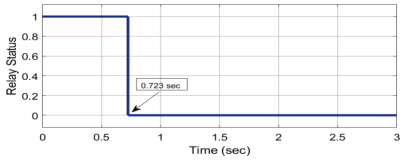

Fig. 16. Tripping status of primary relay R_{16}.

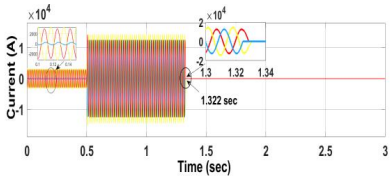

Fig. 17. Fault current and tripping time of backup relay R_9.

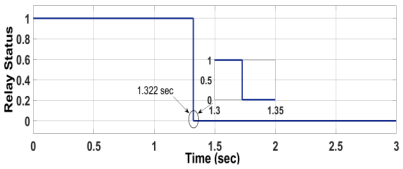

Fig. 18. Tripping status of backup relay R_9.

of the primary relay R_{16} occurs, backup relay R_9 & R_{22} come into action and trip after a CTI difference of 0.6 & 1.66 sec respectively. The performance of backup relays R_9 & R_{22} are shown in Figs. 17-20.

5.2. Islanded mode

In this operating mode, the primary grid is disconnected from the distribution system, and the SBDGs serve as the sole power sources for supplying loads. As a result, the fault current and short circuit level are reduced compared to the grid-connected mode. However, the relay settings suitable for grid-connected mode may

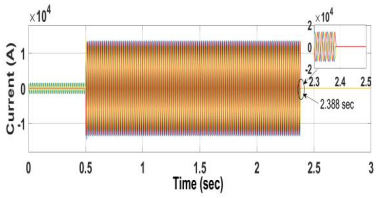

Fig. 19. Fault current and tripping time of backup relay R_{22}.

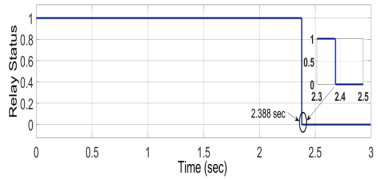

Fig. 20. Tripping status of backup relay R_{22}.

malfunction or misoperate in the islanded operation. To address this, new settings for the relay pairs will be calculated using the proposed adaptive protection algorithm.

Multiple types of faults are imitated at eleven different locations, and the fault current magnitudes are sensed and updated in the relay coordination model. This entails updating the non-linear modified objective function with the new fault current data and processing it to obtain new TDS and CPS values.

A) Single-phase feeder

At point E, a single line to ground fault is simulated. Upon observing the status of the PCC circuit breaker, the MCPC will transit the mode from grid-connected to islanded mode. After receiving the data from IFEDs, the relay programming module will subsequently update the combinations of relay pairs to accommodate the islanded mode. The variations in the fault currents can be seen in Figs. 21 and 23, while Figs. 22 and 24 display the tripping status of the primary and backup relays, respectively.In islanded mode, it is evident that the fault current for a line-to-ground fault is significantly lower, reduced by 58.19% compared to the same fault occurring in grid-connected mode. This decrease in fault magnitude highlights the capability of the proposed scheme to effectively converge towards optimal solutions, providing well-suited values for TDS and CPS for both primary and backup relays.

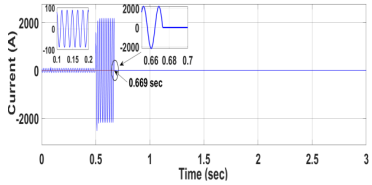

Fig. 21. Fault current and tripping time of primary relay R_{11}.

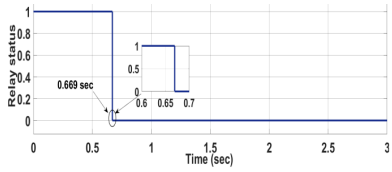

Fig. 22. Tripping status of primary relay R_{11}.

B) Two-phase feeder

The effectiveness of the proposed algorithm is also evaluated for a line-to-line fault occurring at fault point A. The fault current

is solely generated by all three SBDGs. Both the primary relay R_1 and backup relay R_2 experience the fault current in only one direction due to the fault's location at the farthest end of the feeder. The performance of relay R1 and relay R_2 is presented in Figs. 25 to 28.

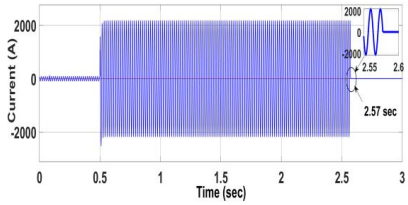

Fig. 23. Fault current and tripping time of backup relay R_{12}.

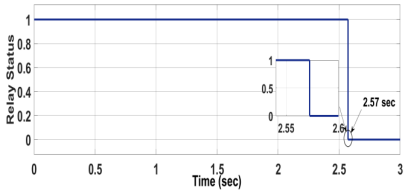

Fig. 24. Tripping status of backup relay R_{12}.

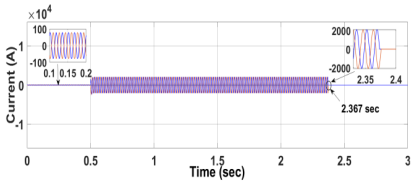

Fig. 25. Fault current and tripping status of primary relay R_1.

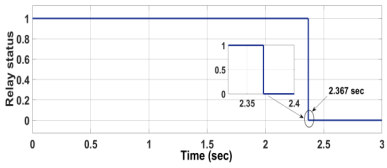

Fig. 26. Tripping status of primary relay R_1.

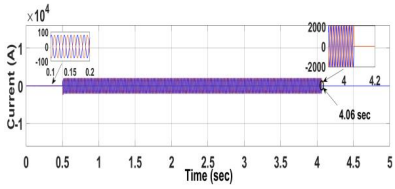

Fig. 27. Fault current and tripping time of backup relay R_2.

The primary relay experiences an 82.24% reduction in fault current compared to grid-connected mode. These results demonstrate the effectiveness of the proposed algorithm in maintaining relay sensitivity even when fault current levels vary. The operating time of primary relay R_1 is 1.86 sec after inception of fault.

The optimized values for TDS and CPS are 0.978 and 0.5, respectively, as compared to 0.1 and 2.5 in the grid-connected

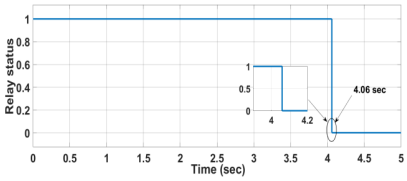

Fig. 28. Tripping status backup relay R_2.

mode. Similarly, the settings of back up relay are calculated and updated in the relay module. In this scenario, the computed CTI is 1.69 seconds, exceeding the minimum required CTI_{min}.

C) Three-phase feeder

A three-phase to-ground bolted fault is simulated at fault point I. The fault current is generated by all the DGs but flows through different directions. In this case, the directional elements integrated into the adaptive relay function effectively discern the fault direction. To ensure network security and maintain reliability, the primary and backup relays are carefully chosen to minimize the disconnection of the network while clearing the fault. Relay R_{16} operates as the primary relay for currents contributed by DG1 and DG3, followed by the backup relay R_{15}. Another relay pair from the DG2 side consists of R_{17} and R_{18}. The tripping times of the relays on both sides of fault point I are depicted in Figs. 30 to 35. These figures provide a comprehensive overview of how the relays operate and respond in the given scenario. Fault current directions contributed from all DGs are shown in Fig. 29. As compared to grid-connected mode, the fault current magnitude in islanded mode is decreased by 84.8%. With this large change in magnitude of fault current, relay requires a new settings for its functionality. The proposed algorithm calculated the new sets of values of TDS and CPS for all relays.

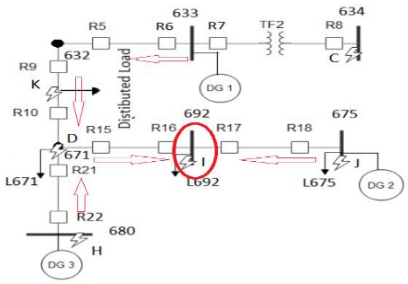

Fig. 29. Fault current contribution from all DGs for fault point I.

The results revealed that all the relay pairs have CTI values above the minimum CTI, except for the primary relay R_{18} and backup relay R_{17} pair, which has a CTI value of 0.284 seconds, very close to CTI_{min}. To prevent miscoordination of this relay pair, the algorithm must reset and recalculate a new set of TDS and CPS values specifically tailored for this pair. It is worth noting that in islanded mode, the CTI of some relay pairs is greater than the CTI in grid-connected mode. This disparity arises due to significant variation in the fault current magnitude between the grid-connected mode and the islanded mode. By increasing the value of β, the level of miscoordination in ANDOCR is reduced. So, this leads to an increase in the operational time of the relays and thus the CTI. The value of β is taken as 100 in both modes of operation.

The primary relay R_{16}, and the backup relay R_{15} have tripping times of 1.647 sec and 2.05 sec respectively. CTI obtained for this relay pair is 0.406 sec. and the second relay pair (R_{17} and R_{18}) gives a CTI of 0.697 sec, which satisfied the constraint limit of CTI.

The optimized values of CTI of all relay pairs are graphically displayed in Fig. 36. Operating time of all primary and backup

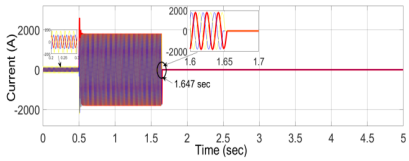

Fig. 30. Fault current and tripping time of primary relay R_{16}.

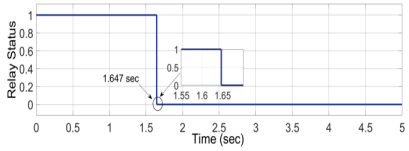

Fig. 31. Tripping status of primary relay R_{16}.

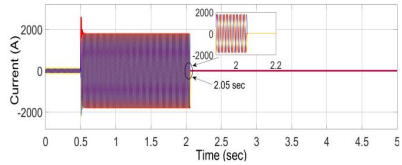

Fig. 32. Fault current and tripping time of backup relay R_{15}.

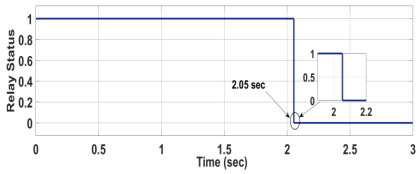

Fig. 33. Tripping status of backup relay R_{15}.

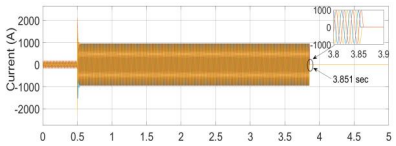

Fig. 34. Fault current and tripping time of primary relay R_{17}.

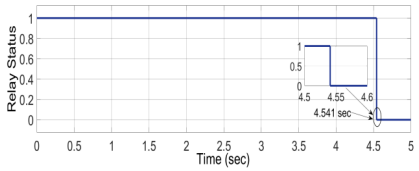

Fig. 35. Tripping status of backup relay R_{18}.

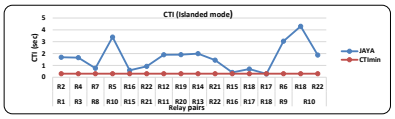

Fig. 36. CTI for all relay pairs in Islanded mode.

relay pairs for various fault points are given in Table 4. All the optimized values of TDS and CPS for islanded mode are graphed in Figs. 37 and 38 respectively.

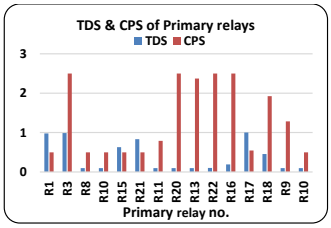

Fig. 37. Optimized TDS and CPS values of primary relays.

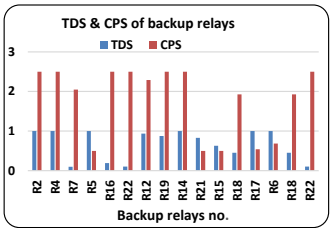

Fig. 38. Optimized TDS and CPS values of backup relays.

5.3. Sensitivity analysis

Coordination of DOCRs is renowned for being a complex nonlinear optimization problem with stringent constraints. In this perspective sensitivity analysis is a critical study to find out the impact of control parameters on outcome. This analysis sought to explore and validate the effects of common control parameters on the sensitivity of the DOCR. JAYA algorithm has only two control parameters,, i.e,, no. of population and no. of iteration. So, focus on the control parameters of the JAYA algorithm by restricting the population to feasible regions and a number of iterations. Regardless of the nature of the optimization problem, specific values and choices for these control parameters have a significant impact on the efficiency of the proposed scheme.

A) Effect of population size

The sensitivity is analyzed by setting the population size to 50, 100, 200, 400,800, and 1000. The behavior of convergence curves with different no. of populations are shown in Fig. 39. When the population size is set at 50, the convergence took more no. of iteration and obtained total operating time of primary relay is 9.31sec. Consequently, when the population size was set at 100, the time multiplier parameters were smaller compared to a population size of 50. This indicates that the overall relay operating time, or speed of operation, was optimized, leading to a system that exhibits improved sensitivity. It is observed that above 100 population size, the convergence took 8 to 25 no. of

Table 4. Operating time of primary and backup relays.

Fault Point	P	OT_P	B	OT_B
A	R_1	1.867	R_2	3.56
B	R_3	1.877	R_4	3.532
C	R_8	0.335	R_7	1.096
D	R_{10}	0.397	R_5	3.791
	R_{15}	2.046	R_{16}	2.632
	R_{21}	3.196	R_{22}	4.155
E	R_{11}	0.169	R_{12}	2.074
F	R_{20}	0.245	R_{19}	2.157
G	R_{13}	0.217	R_{14}	2.215
H	R_{22}	0.941	R_{21}	2.385
I	R_{16}	1.149	R_{15}	1.553
	R_{17}	3.351	R_{18}	4.041
J	R_{18}	2.314	R_{17}	2.598
K	R_9	0.844	R_6	3.887
	R_{10}	0.283	R_{18}	4.586
			R_{22}	2.155
Total Operating Time		19.23 sec		46.41 sec

Table 5. MOF values using probabilistic methods.

Optimization Techniques	MOF in Grid Connected Mode	MOF in Islanded Mode
PSO	56.56	74.70
GSA	49.87	59.04
JAYA	**30.28**	**54.72**

iterations, proving it to be a faster converging algorithm. The sum of operating time of all primary relays with different no. of population size is shown in Fig. 41. The response indicated in Fig. 41 reveals that the primary relays took too long to operate when the population size was set at 50, violating the principle of swiftly isolating faults for protection. This also suggests that protection coordination was not achieved, with some DOCRs violating the relay coordination constraint. On the other hand, when a population size of 100 was employed, optimal protection coordination was satisfactorily achieved within the microgrid. Selectivity was also accomplished, promptly isolating faulty equipment from the system within the specified CTI. A good response with minimal operating time was achieved in the 100-800 population size range. Larger populations require more memory to store the population of solutions, which can be a limitation in memory-constrained environments. Furthermore, a larger population size may slow down the algorithm's convergence.

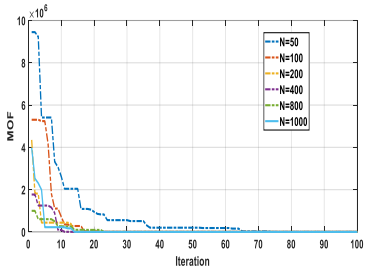

Fig. 39. Effect of population size on proposed scheme.

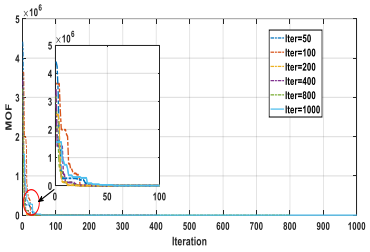

Fig. 40. Effect of iterations on proposed scheme.

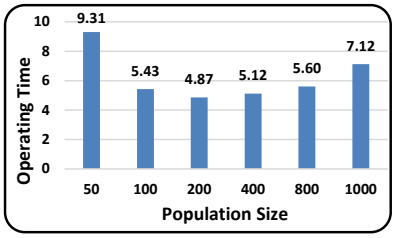

Fig. 41. Total operating time of primary relays with different no. of population size.

B) Effect of number of iterations

In identifying the effect of number of iterations in this sensitivity analysis, we have set the number of iterations at 50,100,200,400,800, and 1000. The convergence characteristics for different no. of iterations are depicted in Fig. 40. It is

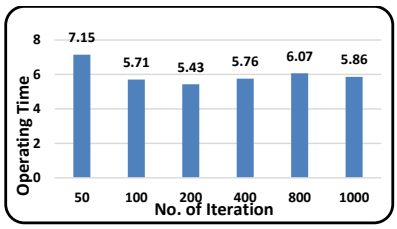

Fig. 42. Total operating time of primary relays with different no. of iteration.

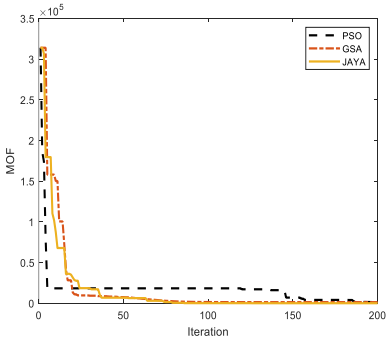

Fig. 43. Convergence characteristics of PSO, GSA, and JAYA in grid-connected mode.

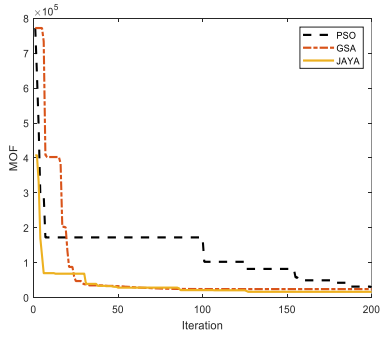

Fig. 44. Convergence characteristics of PSO, GSA and JAYA in islanded mode.

observed that all the cases converge in less than 50 number of iterations. Above it, there is no significant effect on the convergence profile. As the number of iterations increases, it may be problematic when optimizing real-time or time-sensitive processes. It may also increase the computational cost, which can become prohibitive for large-scale problems. Fig. 42 showcases the statistical analysis of the primary relays' net operating times. It is concluded that the minimum operating time is achieved at 200 no. of iteration, which is moderate in size and best suited for this proposed objective function. However, the number of iterations may change with the complexity of objective functions. The operating times achieved by varying the number of iterations are similar across all the relays above the value of 50. Consequently, increasing the number of iterations has an insignificant impact on the proposed algorithm's performance and can sometimes result in unnecessary computational demands. Furthermore, the protection system maintains its selectivity consistently throughout the variations in iterations, and the speed of operation is minimized. The response of the DOCRs demonstrates that increasing the number of iterations does not enhance the efficiency of JAYA, as the algorithm is primarily free from specific control parameters.

The proposed algorithm converges to global optimum values with fewer iterations and less computational time. So, in microgrid

Table 6. Comparison of operating times of primary and backup relays with COF and MOF.

Optimization technique	Grid-connected mode					Islanded mode				
	Total operating time of primary relay (sec)		Total operating time of backup relay (sec)		No. of CTI violations	Total operating time of primary relay (sec)		Total operating time of backup relay (sec)		No. of CTI violations
	COF	MOF	COF	MOF		COF	MOF	COF	MOF	
PSO	17.92	17.02	43.06	42.21	2	29.05	28.126	55.31	54.97	3
GSA	12.02	11.25	37.75	37.36	3	21.43	20.844	44.13	43.42	6
JAYA	5.31	4.82	24.82	24.38	0	19.82	19.231	46.82	46.41	1

Table 7. Comparison of the proposed scheme with previous works.

Reference	Protection Type	Mode of operation(s)	Used Objective function	Technique used on the test system	Relay Setting Mode
[6]	Non-Adaptive	Grid-connected & Islanded	COF	GA-LP on Canadian distribution benchmark and modified IEEE 14 bus (complex approach)	Offline
[7]	Non-Adaptive	Grid-Connected mode	COF	HWOA on IEEE 3 bus, 8bus, nine bus,15 bus, 30 bus (Complex Algorithm)	Offline
[13]	Non-Adaptive	Grid-connected & Islanded	COF	DE algorithm on IEEE 9bus (Simple but parameter sensitive and slow convergence)	Offline
[14]	Adaptive	Grid-Connected mode	No Objective function was used; hence no optimization model	Adaptive with High penetration of DGs in 60 bus distribution feeders (Limited to High penetration of DGs)	Offline
[15]	Adaptive	Grid-connected & Islanded	COF	GA-NLP on 9 bus system (used COF, miscoordination issue)	Online
[26]	Non-Adaptive	Grid-connected & Islanded	No Objective function used No Objective function used hence no optimization model	No optimization technique used (Simple and not adaptive)	Offline, No relay coordination
Proposed Scheme	Adaptive	Grid-connected & Islanded	MOF	JAYA on IEEE 13 node distribution system (simple fast, efficient & algorithm-specific parameters less technique)	Online

protection applications where settings of DOCRs are changed in real-time, this scheme is a perfect option. This study's findings indicate that the appropriate number of population size and iterations depends on the nature and complexity of the problem. A smaller value reduces the likelihood of reaching a global solution, while larger values increase computational efforts.

5.4. Comparative analysis

From all the scenarios, it is concluded that the proposed scheme functions properly in any fault and maintains the coordination adequately. The relay coordination module can adjust the values of TDS and CPS according to the operating conditions. The superiority of the JAYA technique with the proposed objective function over PSO and GSA techniques is evident in its convergence performance. Regardless of the mode of operation of microgrids, JAYA consistently achieves the lowest value for the objective function. The convergence graphs compared to PSO and GSA are shown in Fig. 43 and 44, respectively.

Table 5 provides the optimization results for the proposed objective function of both modes using popular heuristic methods such as PSO, GSA, JAYA for comparison purposes. It is evident that the JAYA technique with MOF has proved its superiority over PSO and GSA techniques in terms of overall operating time in various microgrid modes. Additionally, PSO and GSA probabilistic methods require multiple runs, which can be time-consuming for setting calculations. In the case of adaptive relay where an online setting calculation is necessary, the JAYA method would be a favourable choice as this provides results quickly.

Comparing the total relay operating time in grid-connected and islanded mode (Table 6) with COF MOF both, it is evident that

the settings obtained from JAYA result in a lower operating time than those obtained from PSO and GSA. The net gain in operating time of primary relay with proposed method is 71.7% and 57.15% achieved compared to PSO and GSA respectively. This indicates the faster relay operation while ensuring the fulfillment of all constraints. The scheme proposed in this study is compared to previous research conducted in the field of relay coordination.

The distinctive aspect of the proposed setting is that it enables very well-coordinated tripping of circuit breakers associated with primary and backup relays in both modes, regardless of the scenario. This means that any of the event operation settings ensure proper relay coordination. It is worth emphasizing that the specific features mentioned in Table 7 about the proposed scheme have yet to be covered or examined in prior research.

6. Conclusion

This paper presents an adaptive protection scheme suitable for disparate microgrid operation modes. The viability of the proposed scheme is assessed within the context of the IEEE 13-node distribution system, considering grid-connected and islanded mode. The outcomes of this paper are as follows:

- The performance of the JAYA optimization technique with MOF is proven to be superior over PSO and GSA. The comparative study reveals that the proposed method outperforms PSO and GSA, exhibiting a notable reduction in relay operating times and maintaining the CTI. Specifically, compared to PSO and GSA. The sum of total operating times for primary relays in grid-connected mode is reduced by 71.6% and 57.1%, and in the islanded mode it is reduced by 7.7% and 31.62%, respectively.
- The scheme effectively manages potential miscoordination issues arising from the change in modes of operation. The proposed MOF for the relay coordination problem in a microgrid scenario yields better coordination than COF.
- This proposed technique yielded an impressive and rapid convergence rate, achieving its optimal value within the 37% and 45% of its maximum iterations in grid-connected mode and islanded mode, respectively.
- By systematically modifying one parameter at a time while maintaining others as constant, the proposed scheme is able to pinpoint the parameter responsible for inadequate protection selectivity and operational speed.

The effective protection coordination of relays in different microgrid operating modes confirm the viability and reliability of the proposed protection scheme.

References

[1] I. E. Commission, "International electrotechnical vocabulary." http://www.electropedia.org., 1950.

[2] E. Hayden, "Introduction to microgrids," *Securicon: Alexandria, VA, USA*, 2013.

[3] N. Hatziargyriou, *Microgrids: architectures and control*. John Wiley & Sons, 2014.

[4] N. Kumar, S. Dahiya, and K. Parmar, "Sensitivity analysis based multi-objective economic emission dispatch in microgrid," *J. Oper. Autom. Power Eng.*, 2023.

[5] H. Louie, G. Goldsmith, P. Dauenhauer, and R. H. Almeida, "Issues and applications of real-time data from off-grid electrical systems," in *2016 IEEE PES PowerAfr.*, pp. 88–92, IEEE, 2016.

[6] H. Al-Nasseri and M. Redfern, "Harmonics content based protection scheme for micro-grids dominated by solid state converters," in *2008 12th Int. Middle-East Power Syst. Conf.*, pp. 50–56, IEEE, 2008.

[7] T. S. Aghdam and H. K. Karegar, "Relay curve selection approach for microgrid optimal protection," *Int. J. Renewable Energy Res.*, vol. 7, no. 2, pp. 636–642, 2017.

[8] T. Khurshaid, A. Wadood, S. G. Farkoush, J. Yu, C.-H. Kim, and S.-B. Rhee, "An improved optimal solution for the directional overcurrent relays coordination using hybridized whale optimization algorithm in complex power systems," *IEEE Access*, vol. 7, pp. 90418–90435, 2019.

[9] M. A. Haj-Ahmed and M. S. Illindala, "Intelligent coordinated adaptive distance relaying," *Electr. Power Syst. Res.*, vol. 110, pp. 163–171, 2014.

[10] M. A. Zamani, A. Yazdani, and T. S. Sidhu, "A communication-assisted protection strategy for inverter-based medium-voltage microgrids," *IEEE Trans. Smart Grid*, vol. 3, no. 4, pp. 2088–2099, 2012.

[11] E. Sortomme, S. Venkata, and J. Mitra, "Microgrid protection using communication-assisted digital relays," *IEEE Trans. Power Delivery*, vol. 25, no. 4, pp. 2789–2796, 2009.

[12] H. F. Habib, C. R. Lashway, and O. A. Mohammed, "A review of communication failure impacts on adaptive microgrid protection schemes and the use of energy storage as a contingency," *IEEE Trans. Ind. Appl.*, vol. 54, no. 2, pp. 1194–1207, 2017.

[13] R. Graziano, V. Kruse, and G. Rankin, "Systems analysis of protection system coordination: A strategic problem for transmission and distribution reliability," *IEEE Trans. Power Delivery*, vol. 7, no. 2, pp. 720–726, 1992.

[14] A. Sharma and B. K. Panigrahi, "Phase fault protection scheme for reliable operation of microgrids," *IEEE Trans. Ind. Appl.*, vol. 54, no. 3, pp. 2646–2655, 2017.

[15] S. M. Brahma and A. A. Girgis, "Development of adaptive protection scheme for distribution systems with high penetration of distributed generation," *IEEE Trans. Power Delivery*, vol. 19, no. 1, pp. 56–63, 2004.

[16] A. Srivastava and S. K. Parida, "Adaptive protection strategy in a microgrid under disparate operating modes," *Electr. Power Compon. Syst.*, vol. 48, no. 8, pp. 781–798, 2020.

[17] N. Kumar and D. Jain, "An adaptive inverse-time overcurrent protection method for low voltage microgrid," in *2020 IEEE 9th Power India Int. Conf. (PIICON)*, pp. 1–5, IEEE, 2020.

[18] S. D. Saldarriaga-Zuluaga, J. M. López-Lezama, and N. Muñoz-Galeano, "Adaptive protection coordination scheme in microgrids using directional over-current relays with non-standard characteristics," *Heliyon*, vol. 7, no. 4, 2021.

[19] M. N. Alam, S. Chakrabarti, and A. K. Pradhan, "Protection of networked microgrids using relays with multiple setting groups," *IEEE Trans. Ind. Inf.*, vol. 18, no. 6, pp. 3713–3723, 2021.

[20] A. Ataee-Kachoee, H. Hashemi-Dezaki, and A. Ketabi, "Optimized adaptive protection coordination of microgrids by dual-setting directional overcurrent relays considering different topologies based on limited independent relays setting groups," *Electr. Power Syst. Res.*, vol. 214, p. 108879, 2023.

[21] P. Omidi, S. Abazari, and S. Madani, "Optimal coordination of directional overcurrent relays for microgrids using hybrid interval linear programming-differential evolution," *J. Oper. Autom. Power Eng.*, vol. 10, no. 2, pp. 122–133, 2022.

[22] H. Shad, M. Gandomkar, and J. Nikoukar, "An improved optimal protection coordination for directional overcurrent relays in meshed distribution networks with dg using a novel truth table," *J. Oper. Autom. Power Eng.*, vol. 11, no. 3, pp. 151–161, 2023.

[23] M. Faghihi Rezaei, M. Gandomkar, and J. Nikoukar, "Optimizing multi-objective function for user-defined characteristics relays and size of fault current limiters in radial networks with renewable energy sources," *J. Oper. Autom. Power Eng.*, vol. 12, no. 1, pp. 42–53, 2024.

[24] P. Naveen and P. Jena, "Adaptive protection scheme for microgrid with multiple point of common couplings," *IEEE Syst. J.*, vol. 15, no. 4, pp. 5618–5629, 2020.

[25] A. Y. Hatata, M. A. Essa, and B. E. Sedhom, "Adaptive protection scheme for freedm microgrid based on

convolutional neural network and gorilla troops optimization technique," *IEEE Access*, vol. 10, pp. 55583–55601, 2022.

[26] S. D. Saldarriaga-Zuluaga, J. M. López-Lezama, and N. Muñoz-Galeano, "Optimal coordination of over-current relays in microgrids using unsupervised learning techniques," *Appl. Sci.*, vol. 11, no. 3, p. 1241, 2021.

[27] M. A. Anthony, "Electric power system protection and coordination: a design handbook for overcurrent prorection," *McGraw-Hill Companies*, 1995.

[28] P. P. Bedekar and S. R. Bhide, "Optimum coordination of directional overcurrent relays using the hybrid ga-nlp approach," *IEEE Trans. Power Delivery*, vol. 26, no. 1, pp. 109–119, 2010.

[29] A. J. Urdaneta, R. Nadira, and L. P. Jimenez, "Optimal coordination of directional overcurrent relays in interconnected power systems," *IEEE Trans. Power Delivery*, vol. 3, no. 3, pp. 903–911, 1988.

[30] Z. Moravej, F. Adelnia, and F. Abbasi, "Optimal coordination of directional overcurrent relays using nsga-ii," *Electr. Power Syst. Res.*, vol. 119, pp. 228–236, 2015.

[31] A. J. Urdaneta, H. Restrepo, S. Marquez, and J. Sanchez, "Coordination of directional overcurrent relay timing using linear programming," *IEEE Trans. Power Delivery*, vol. 11, no. 1, pp. 122–129, 1996.

[32] J. Moirangthem, K. KR, S. S. Dash, and R. Ramaswami, "Adaptive differential evolution algorithm for solving non-linear coordination problem of directional overcurrent relays," *IET Gener. Transm. Distrib.*, vol. 7, no. 4, pp. 329–336, 2013.

[33] R. Sitharthan, M. Geethanjali, and T. K. S. Pandy, "Adaptive protection scheme for smart microgrid with electronically coupled distributed generations," *Alexandria Eng. J.*, vol. 55, no. 3, pp. 2539–2550, 2016.

[34] F. E. Postigo Marcos, C. Mateo Domingo, T. Gomez San Roman, B. Palmintier, B.-M. Hodge, V. Krishnan, F. de Cuadra García, and B. Mather, "A review of power distribution test feeders in the united states and the need for synthetic representative networks," *Energies*, vol. 10, no. 11, p. 1896, 2017.

[35] W. H. Kersting, "Radial distribution test feeders," *IEEE Trans. Power Syst.*, vol. 6, no. 3, pp. 975–985, 1991.

[36] R. Rao, "Jaya: A simple and new optimization algorithm for solving constrained and unconstrained optimization problems," *Int. J. Ind. Eng. Comput.*, vol. 7, no. 1, pp. 19–34, 2016.